IMPERIAL

Spanwise non-uniform surface temperature distributions for high-speed boundary layer transition control

Dr Paul Bruce, Department of Aeronautics, Imperial College London

ERCOFTAC Autumn Festival, 10 October 2024

With credit to: **Kazuki Ozawa**, **Dr Luca Boscagli**
Funding from: Nakajima Foundation, QinetiQ (WSRF task 0105)
HPC time on ARCHER2 provided by EPSRC (UKTC)

Contents

Background

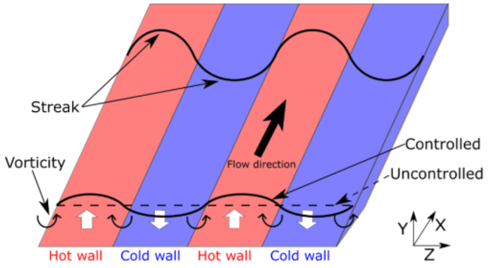

Experimental setup and thermal modelling

Prediction and measurement results

Conclusion

Background
Hypersonic vehicles

Challenges for hypersonic aircraft, missiles, re-entry vehicles, rockets, etc.

- Significant friction drag and aerodynamic heating on vehicles.
- Improving the agility of vehicles is key to control stability.
- Thermal protection systems are required.

HERMEUS Co. (2022)
https://www.hermeus.com/

AIR FORCE. (2022). *X-51A Waverider*
https://www.af.mil/About-Us/Fact-Sheets/Display/Article/104467/x-51a-waverider/

JAXA. (2022). *Orbital Re-entry Experiment (OREX).*
https://global.jaxa.jp/projects/rockets/orex/index.html

Background
Impact on friction and heating

Reynolds analogy

$$\frac{Cf}{2} = St$$

Heat flux

$$q = f(St, T_{bl}, T_w)$$

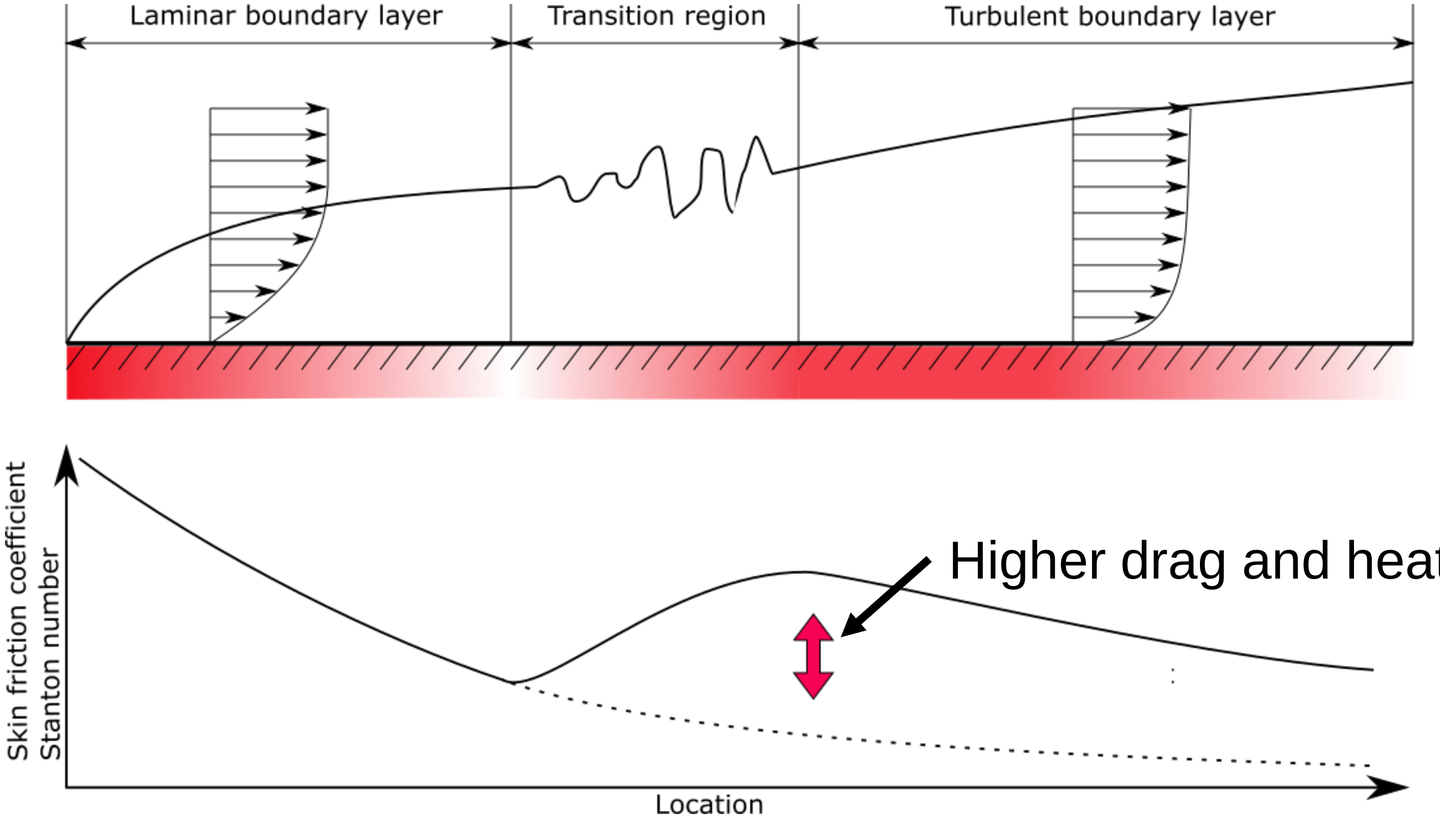

Higher drag and heat flux

Delay transition to reduce drag and heat transfer

Background
Hypersonic transition fundamentals

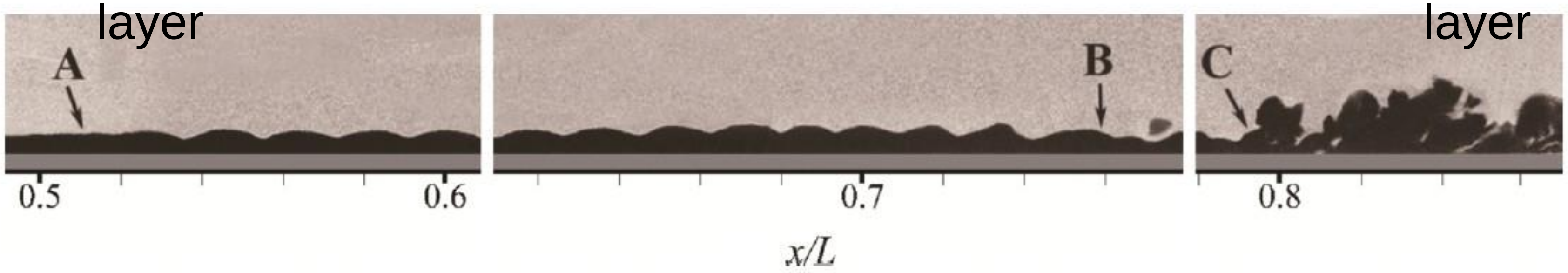

Visualization of hypersonic boundary layer transition [2]

- Hypersonic transition: five modes [3].
- The second mode, Mack mode, is a dominant instability [1-3].
  - Growth of planar acoustic wave.
  - Formed in the shape of 2 ropes in the laminar boundary.
  - Breakdown, and then transition.

[1] C. Zhang, Y. Zhu, X. Chen, H. Yuan, J. Wu, S. Chen, C. Lee, and M. Gad-el Hak, 2015.
[2] L. M. Mack, 1984.
[3] S. Laurence, A. Wagner, and K. Hannemann, 2016.

Background
Previous transition control research

Hypersonic flow over a cone

M_{in}=6

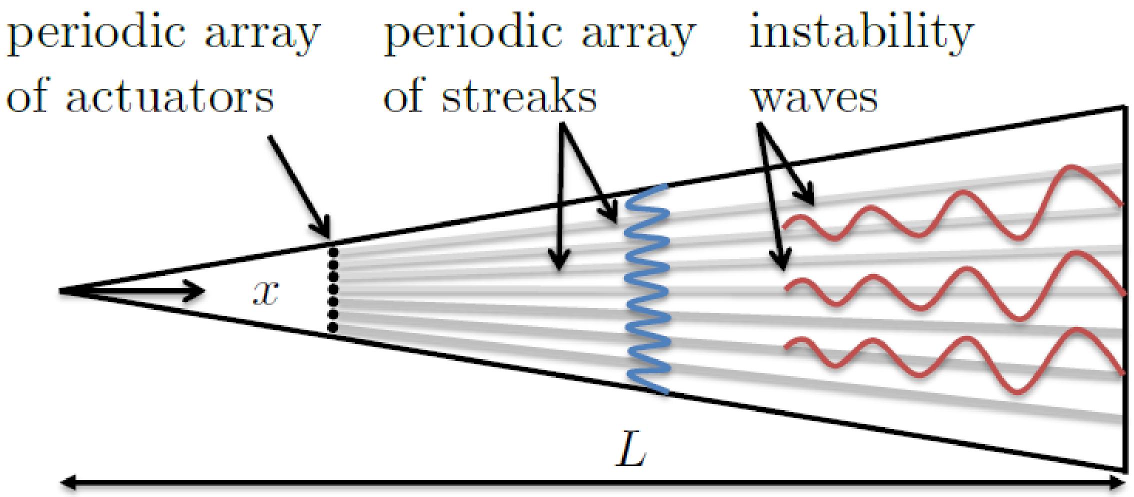

Paredes et al. (2016)

- Effect of periodic array of finite amplitude streaks on Mack modes instability
- Linear (quasi-parallel) boundary layer stability studies
- Streaks can delay transition
  - 2^{nd} (2D) mode is stabilized
  - 1^{st} (3D) mode destabilized, can limit extent of transition delay

Background

Importance of velocity streaks

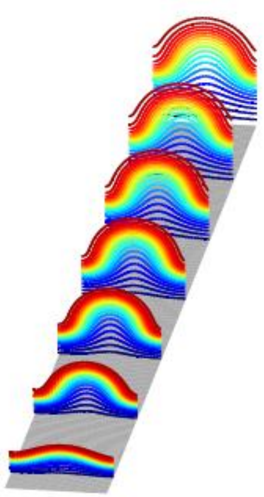

Streak [4]

Possible to delay the breakdown of the 2nd (Mack) mode by streaks [4, 7]

Velocity streaks generation methods

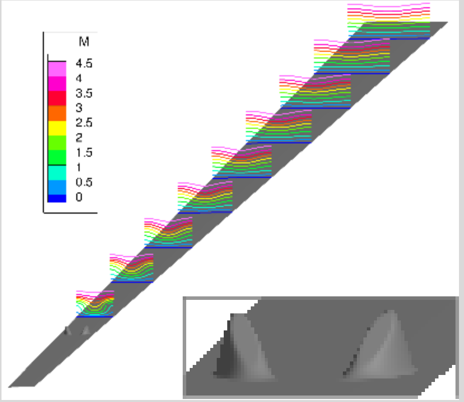

Vortex Generator [5]

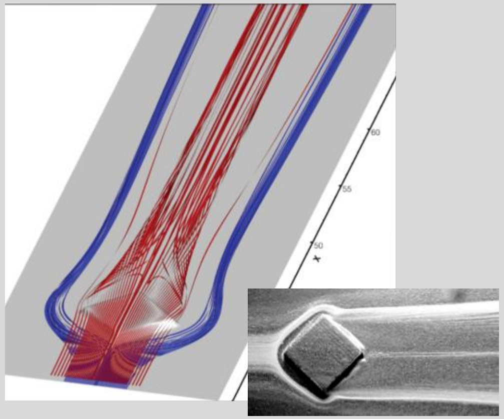

Roughness element [6, 8]

Challenges

- Drag source at off-design conditions
- Lead to early transition when the disturbance is low
- Patch gets damaged under long heating exposure

[4] P. Paredes, M. M. Choudhari, and F. Li, 2016.
[5] P. Paredes, M. M. Choudhari, and F. Li, 2018.
[6] O. Taylor, 2019.
[7] J. Ren, S. Fu, and A. Hanifi, 2016.
[8] P. Balakumar and M. Kegerise, 2016

Background

Generating streaks using non-uniform thermal boundaries

Low speed [9]

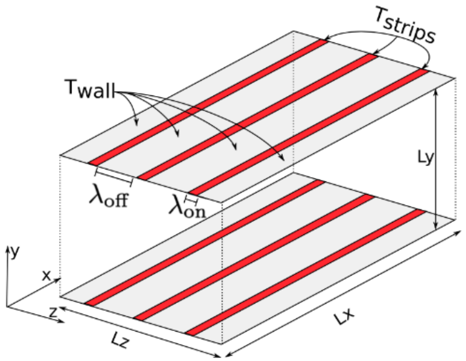

Numerical domain of non-uniform surface temperature boundary conditions

Lift-up mechanism

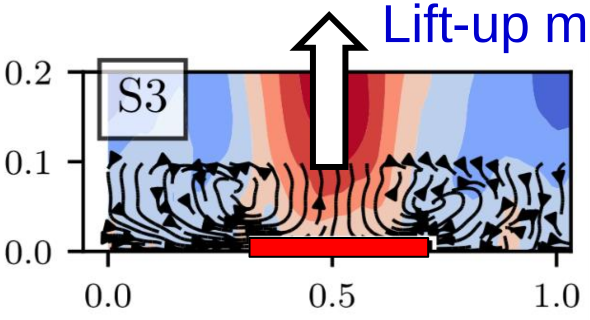

Streamline in the YZ plane

Hypersonic Mach 6 [10]

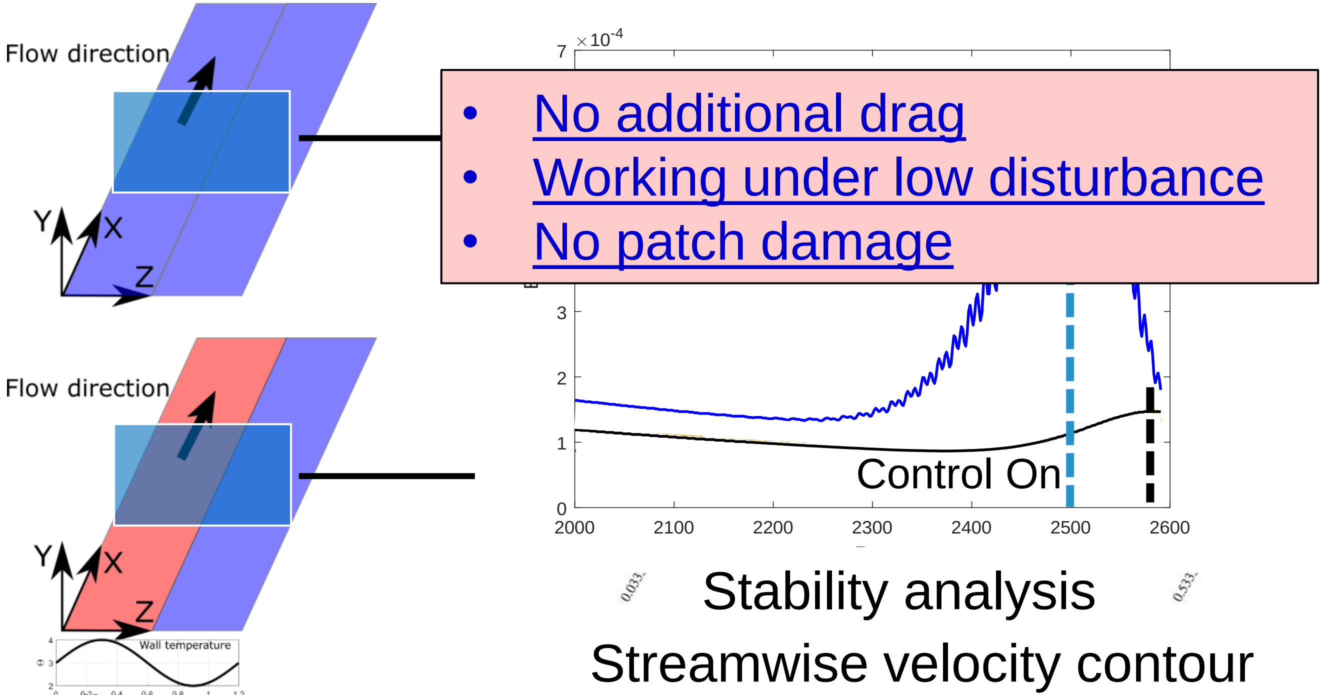

- No additional drag
- Working under low disturbance
- No patch damage

Wall temperature

Stability analysis

Streamwise velocity contour

- A control concept by non-uniform temperature distributions
- DNS to explain the principles behind the concept

[9] J.P. Hickey, K. Younes, M. X. Yao, D. Fan, and J. Mouallem, 2020.
[10] K. Ozawa. C. Xia, G. Rigas and P. Bruce, 2022.

Background

Anticipated impact of control on boundary layer instabilities

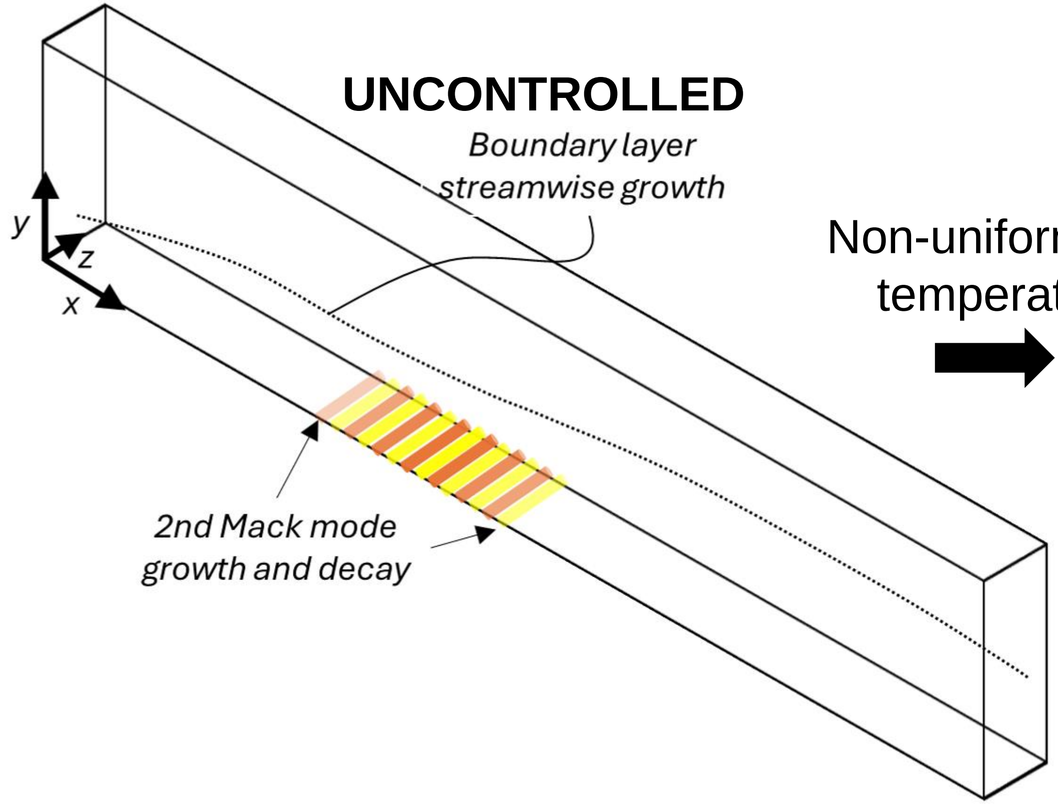

Non-uniform wall temperature

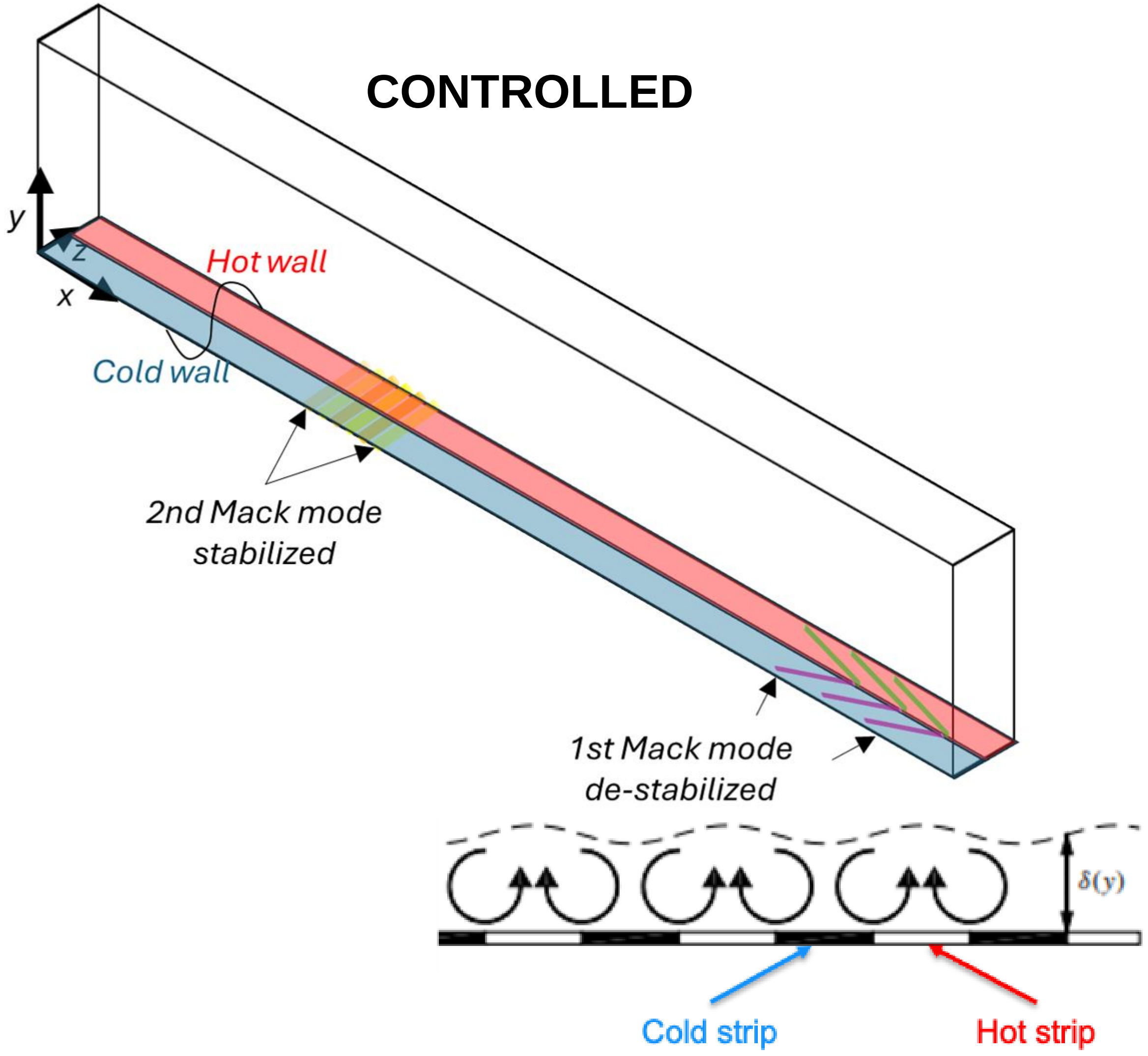

Paul Bruce | p.bruce@imperial.ac.uk

Background

Aims of this research

Concept

↓

Preliminary design

↓

Temperature performance test

↓

Velocity streak performance test

Using the Imperial College supersonic wind tunnel:

1. Evaluation of passive surface temperature distributions using IRT
2. Evaluation of velocity streak generation using LDA

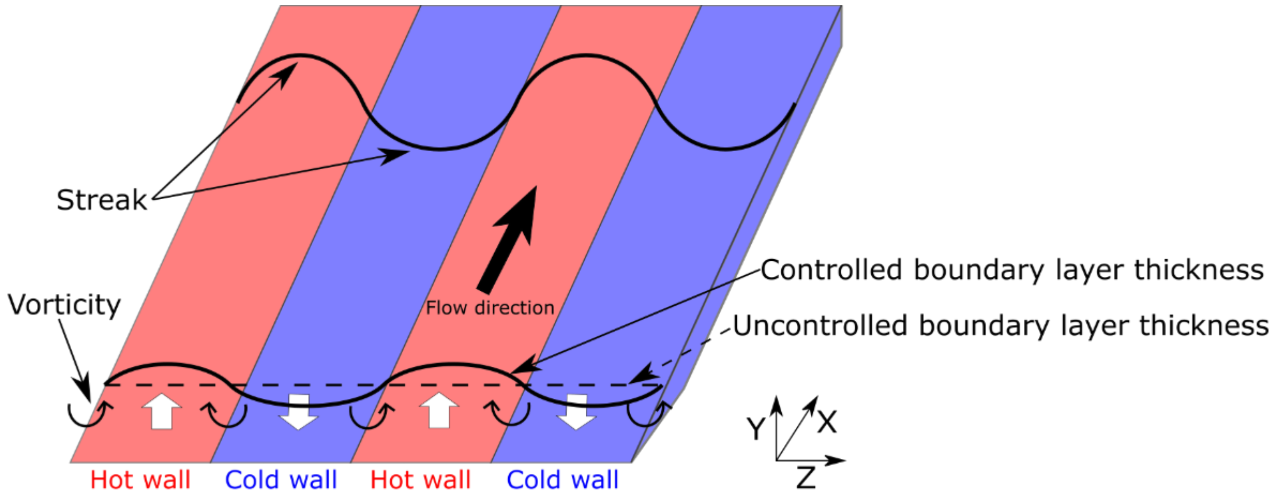

- Flat plate configuration
  - Non-uniform spanwise temperature distribution

Background

Experimental setup and thermal modelling

Prediction and measurement results

Conclusion

Experimental setup and thermal modelling
Experimental apparatus

- Imperial College supersonic wind tunnel (cold tunnel)
- IRT to measure temperature

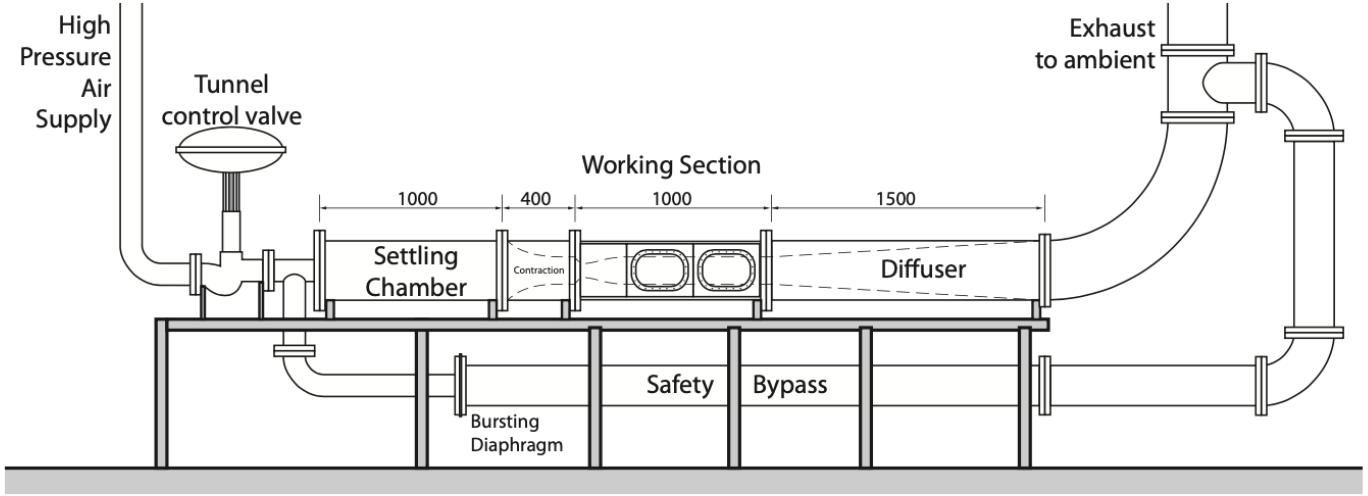

Schematic diagram of the Imperial College supersonic wind tunnel

Freestream condition

M	$Re(\mathrm{m}^{-1})$	$P_\infty(\mathrm{Pa})$	$T_\infty(\mathrm{K})$	$T_r(\mathrm{K})$
2.73	3.7×10^7	15900	117	274

Experimental setup and thermal modelling

Passive control method to generate non-uniform temperature distributions

Heat transfer equation

$$\frac{\partial T}{\partial t} = \frac{\alpha}{\rho c} \nabla^2 T$$

$$= \kappa \left(\frac{\partial^2 T}{\partial x^2} + \frac{\partial^2 T}{\partial y^2} + \frac{\partial^2 T}{\partial z^2} \right)$$

Experimental setup and thermal modelling

Design of the flat plate test article

Dissimilar thermal properties
- Copper
- Ceramic(MACOR)

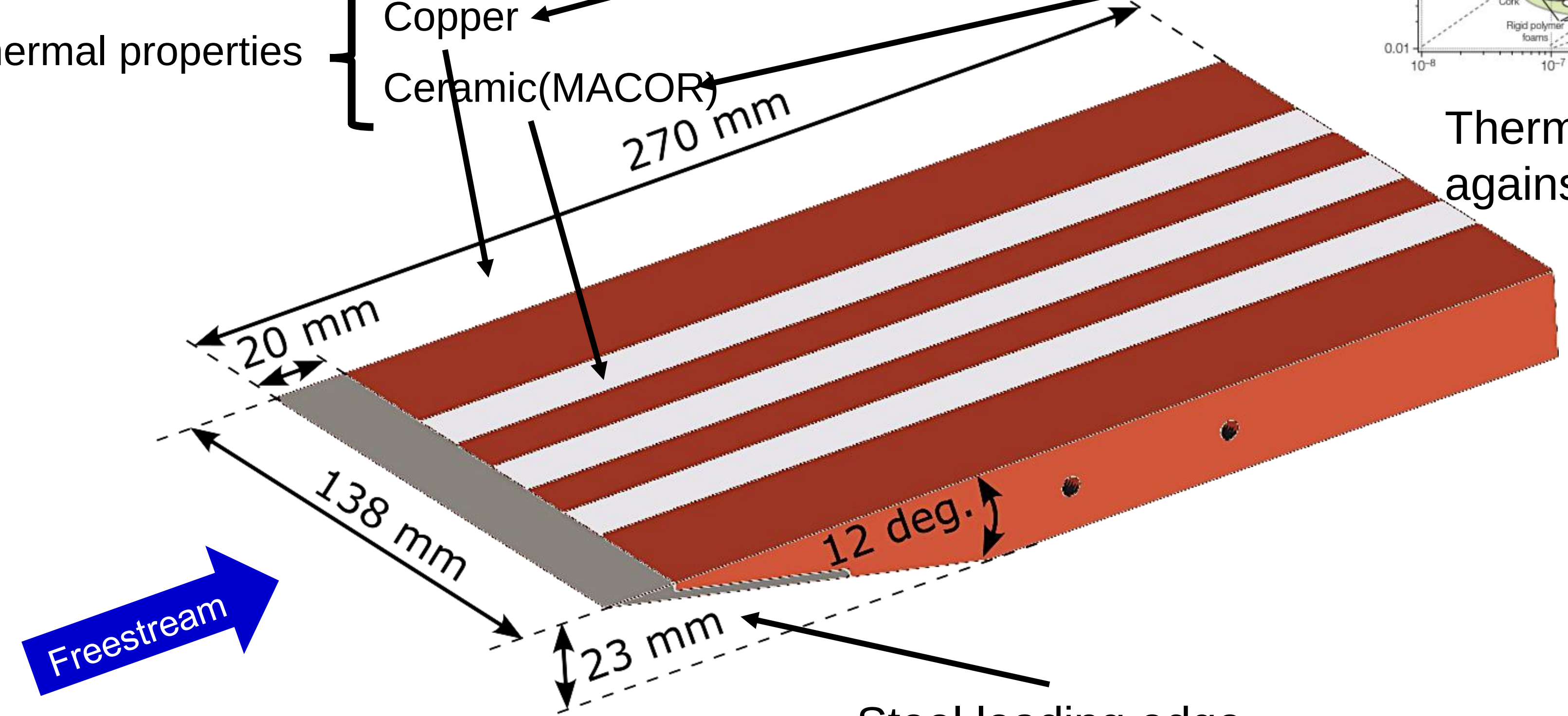

Steel leading edge

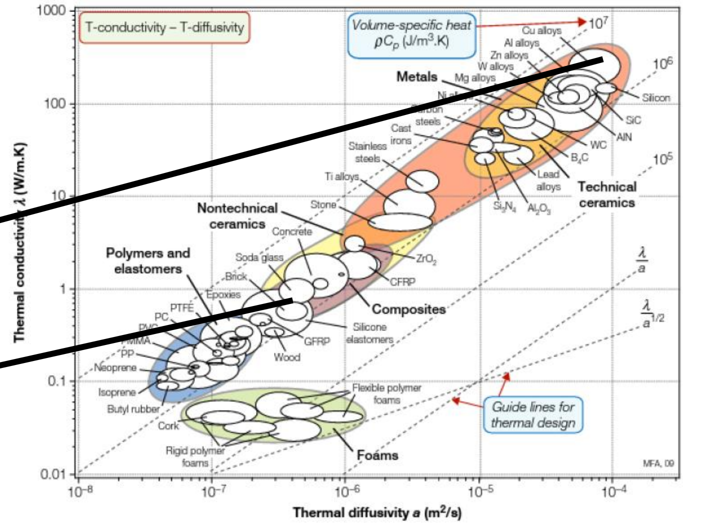

Thermal conductivity plotted against thermal diffusivity [11]

[11] M. F. Ashby, 2017.

Experimental setup and thermal modelling

Heat transfer generation method at cold tunnel

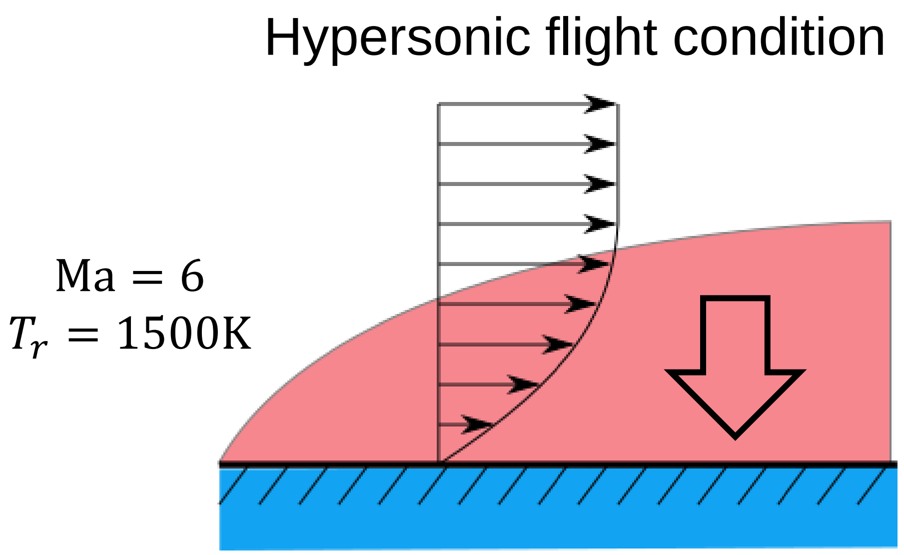

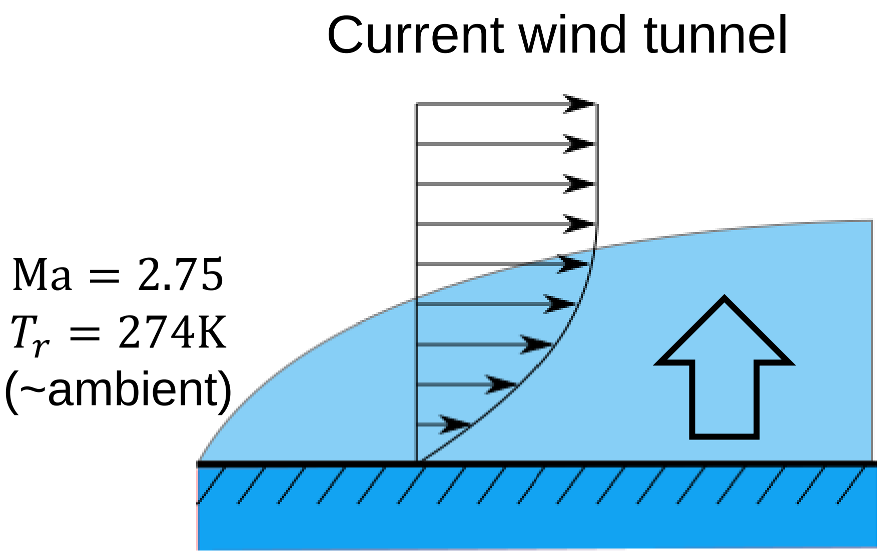

Experimental setup and thermal modelling

Heating system

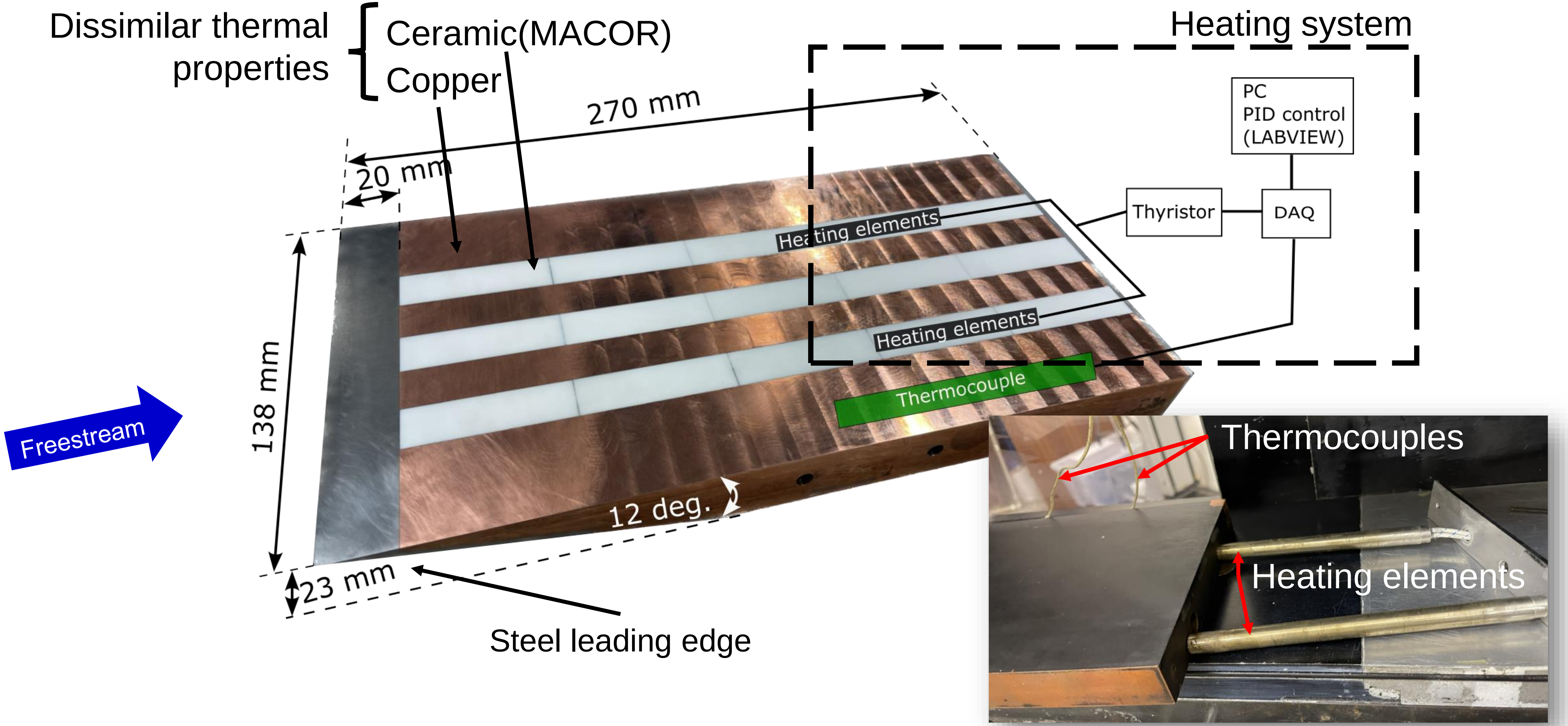

Experimental setup and thermal modelling

Manufactured prototype copper test article

Coating for smooth surface and stable measurement

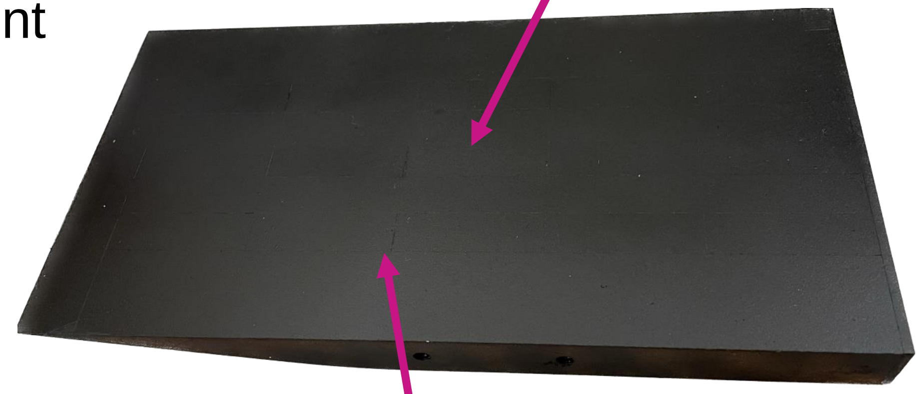

1. An etch primer to enhance the adhesion
2. A heat-resistant paint

- Smooth the surface by polishing the paints
- Thickness is 23μm
- High emissivity (>0.84)

Experimental setup and thermal modelling

Mounting the plate in the test section

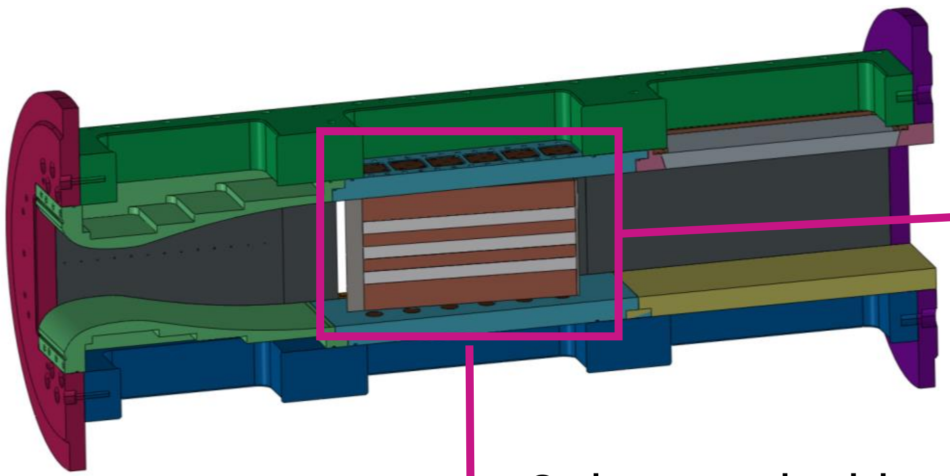

3 degrees incident angle

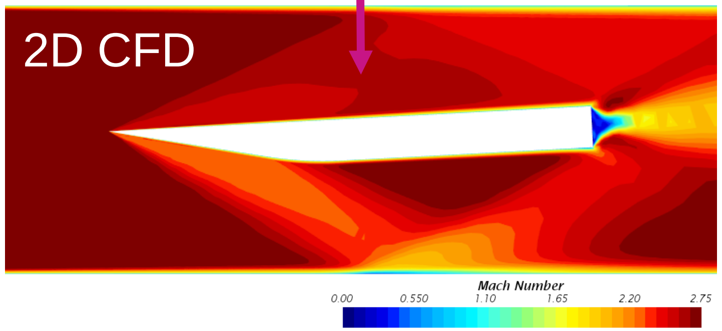

Effective freestream condition

M_2	$Re(\mathrm{m}^{-1})$	$P_{\infty 2}(\mathrm{Pa})$	$T_{\infty 2}(\mathrm{K})$	$T_{r2}(\mathrm{K})$
2.6	3.8×10^7	20000	124	275

Experimental setup and thermal modelling

Infrared thermography (IRT)

- Thin-film gauges and thermocouples prevent heat convection from boundary layer
- IRT provides non-intrusive and high-resolution surface temperature measurements

FLIR A655SC

Detector	Uncooled microbolometer
Spectral response	7.5 – 14 μm
Field of view (FOV)	25°
Resolution	640 x 480
Frame rate	50 Hz
Spatial resolution	6 px/mm

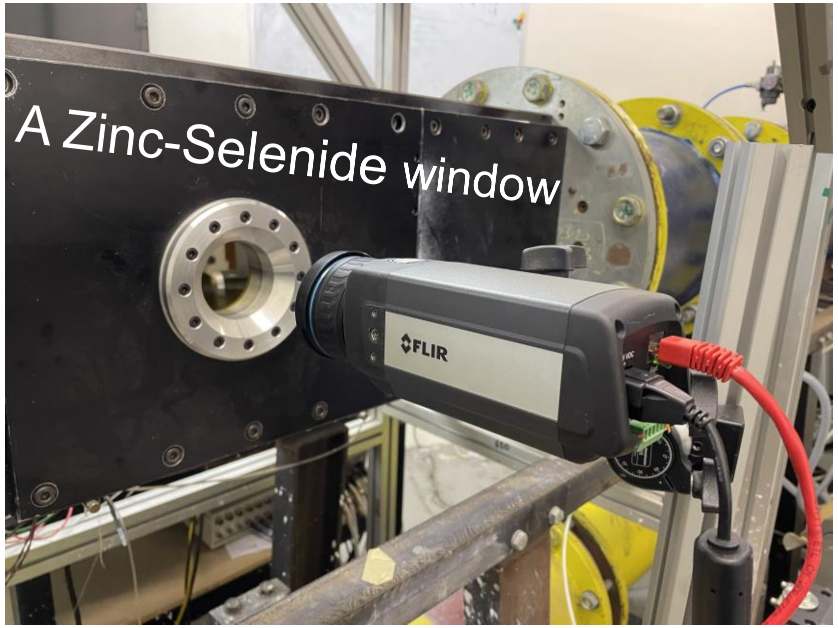

Experimental setup and thermal modelling

In-situ calibration for temperature fitting

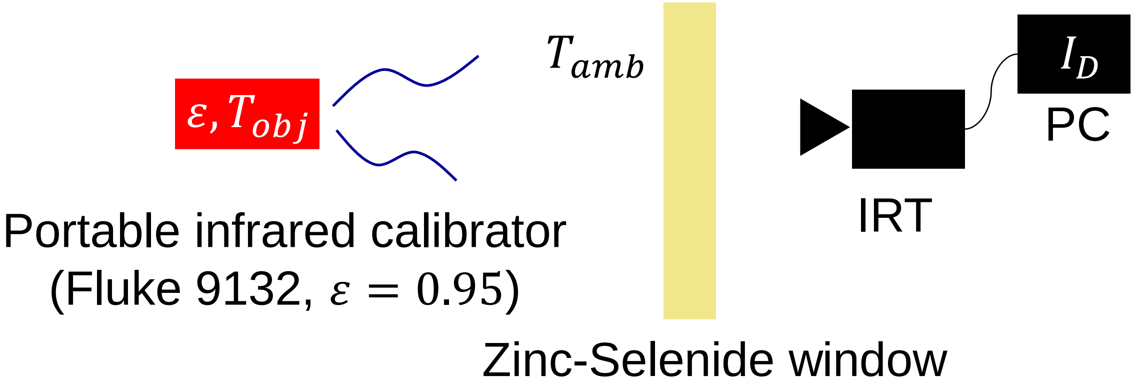

$$I_D = \varepsilon \frac{R}{e^{B/T_{obj}} - F} + (1 - \varepsilon) \frac{R}{e^{B/T_{amb}} - F} + C$$

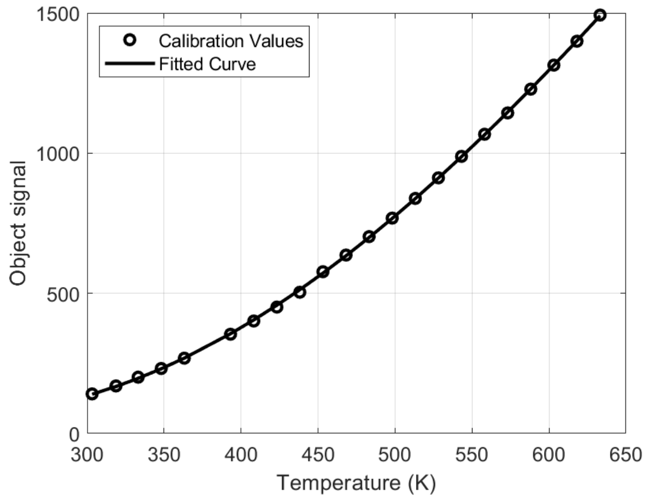

Fitted parameter	value
R	14794
B	1500
F	1.0
C	35.7
Coefficient of determination	0.99
RMS error	3.27

Experimental setup and thermal modelling

In-situ calibration for the paints

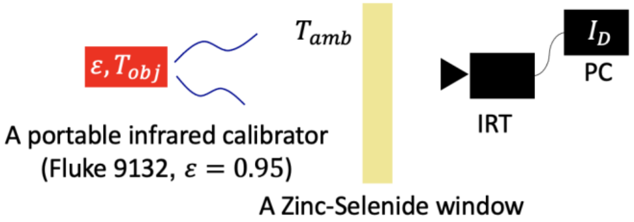

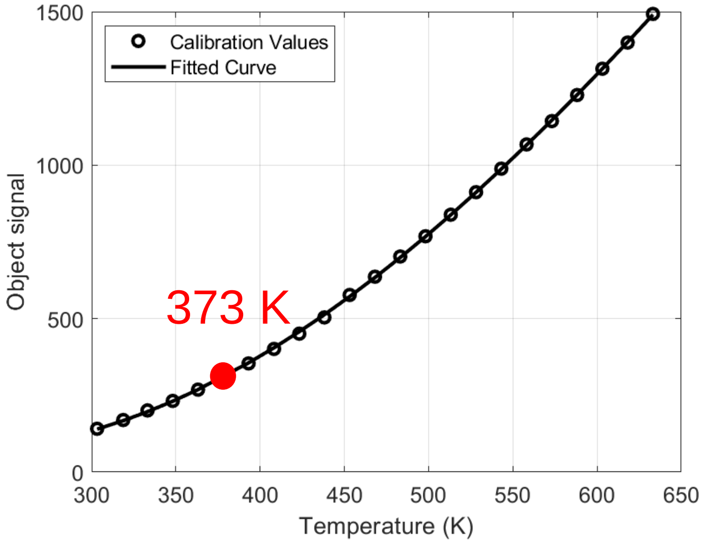

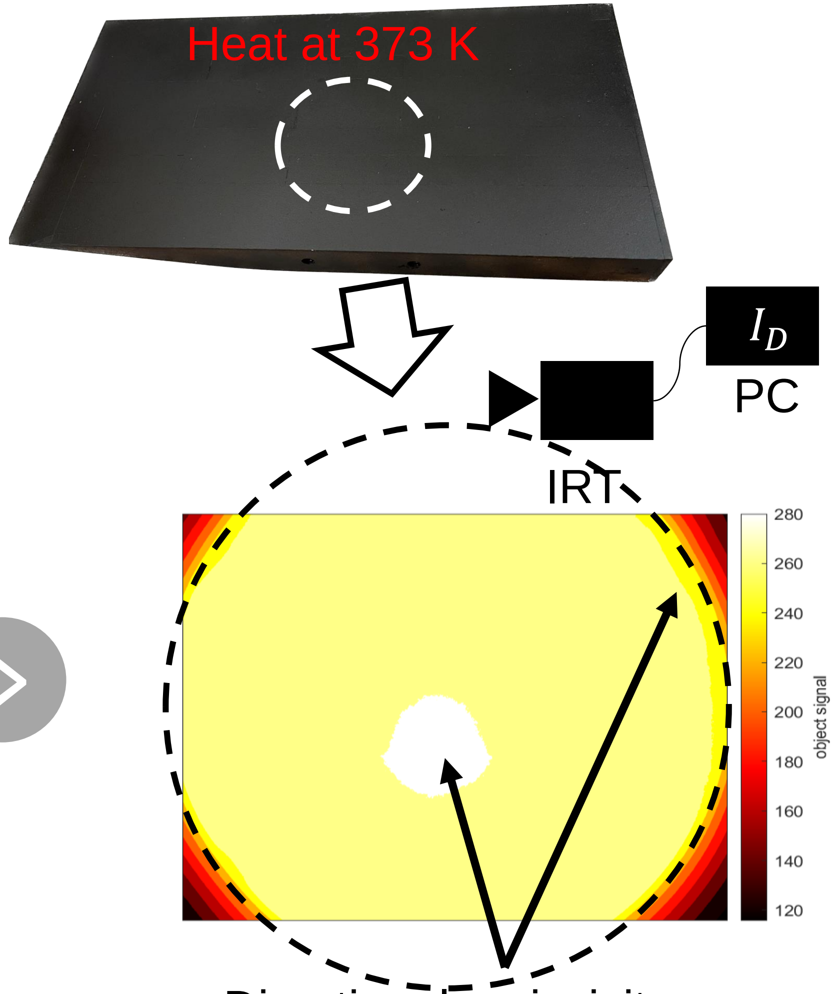

Optimise parameter of R, B, F, C

$$I_D = \varepsilon \frac{R}{e^{B/T_{obj}} - F} + (1 - \varepsilon) \frac{R}{e^{B/T_{amb}} - F} + C$$

- Directional emissivity
- Reflection between the camera lens and the window

Detect ε at each pixel

$$I_D = \varepsilon \frac{R}{e^{B/T_{obj}} - F} + (1 - \varepsilon) \frac{R}{e^{B/T_{amb}} - F} + C$$

Experimental setup and thermal modelling

Spatial calibration

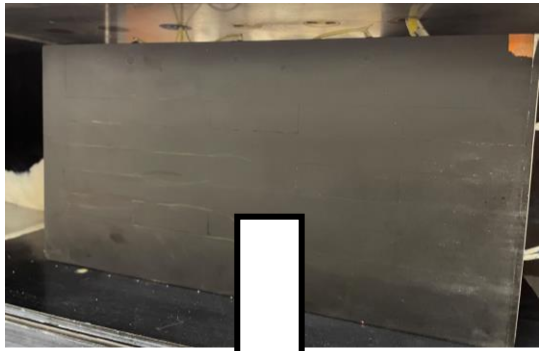

Steel: Low emissivity

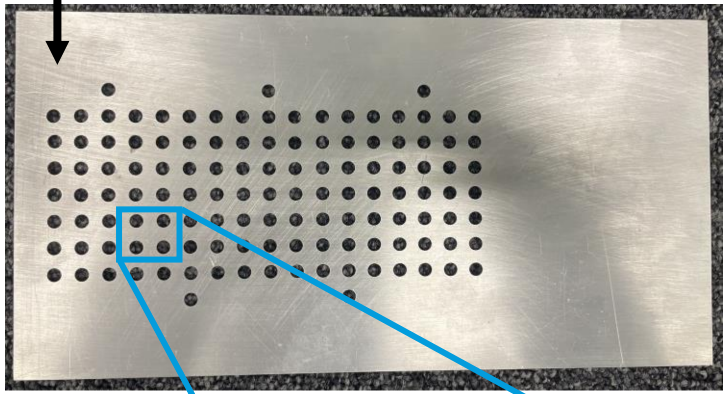

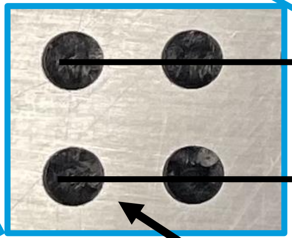

10 mm

D = 5 mm

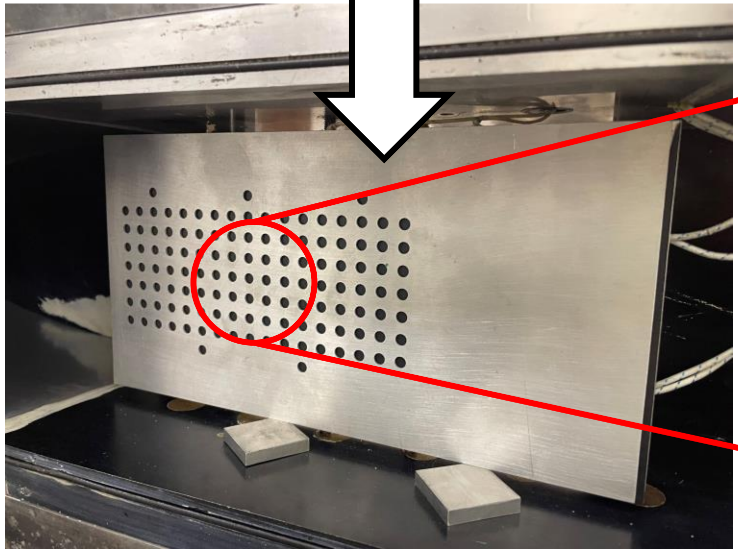

Identify measurement location

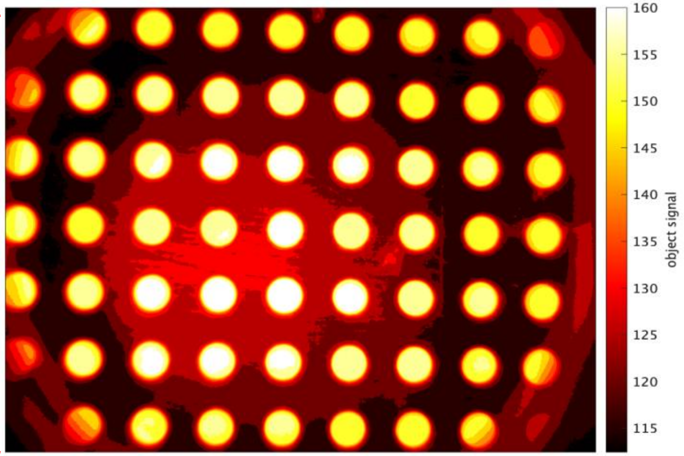

Image captured by IRT

Experimental setup and thermal modelling

Thermal modelling

$$t_{modelling} = -1.5\ [s]$$

Material properties
- Steel
- Ceramic
- Copper

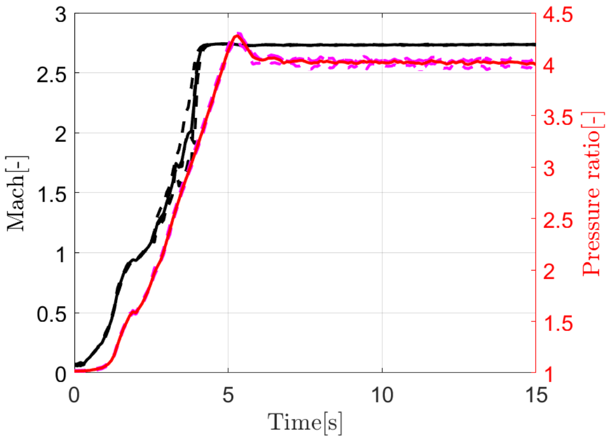

The wind tunnel log

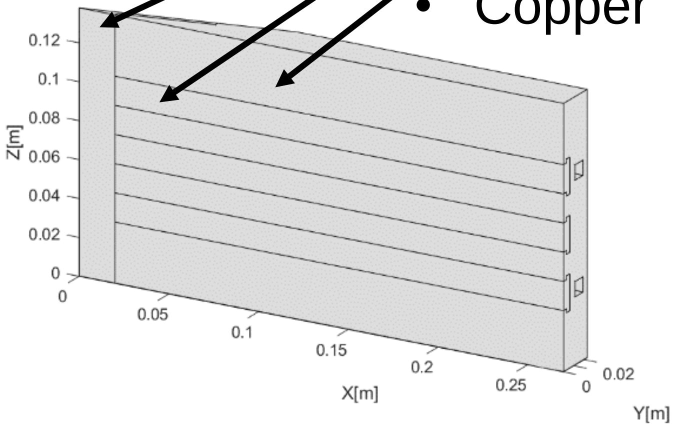

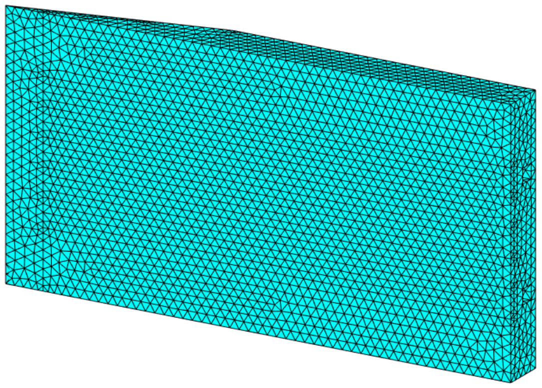

Mesh resolution: 5mm

Boundary condition

$$Heat\ Flux = h_x(T_{bl} - T_w)$$

$$\hookrightarrow h_x = St_x(\rho_{ref} U_\infty C_p)$$

$$\hookrightarrow St_x = \frac{0.0296}{\sqrt[5]{Re_x}} Pr^{-0.67}$$

St_x: The Chilton-Colburn analogy

T_{ref} : The Meador-Smart method

Background

Experimental setup and thermal modelling

Prediction and measurement results

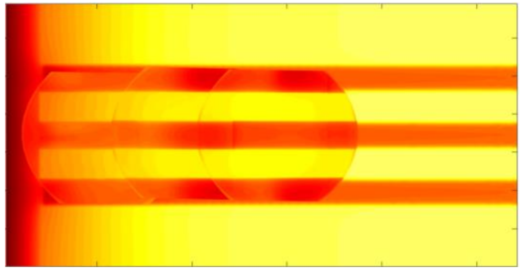

Conclusion

Prediction and measurement results
Test cases and initial conditions

Case	Number of measurements	T_{target}[K]	T_{int}[K]	$T_{target} - T_{int}$[K]	Temperature drop [%]
Case323K	3	323.2	319.5	3.7	7.4
Case373K	3	373.2	362.1	11.1	11.1
Case423K	2	423.2	404.6	18.5	12.3

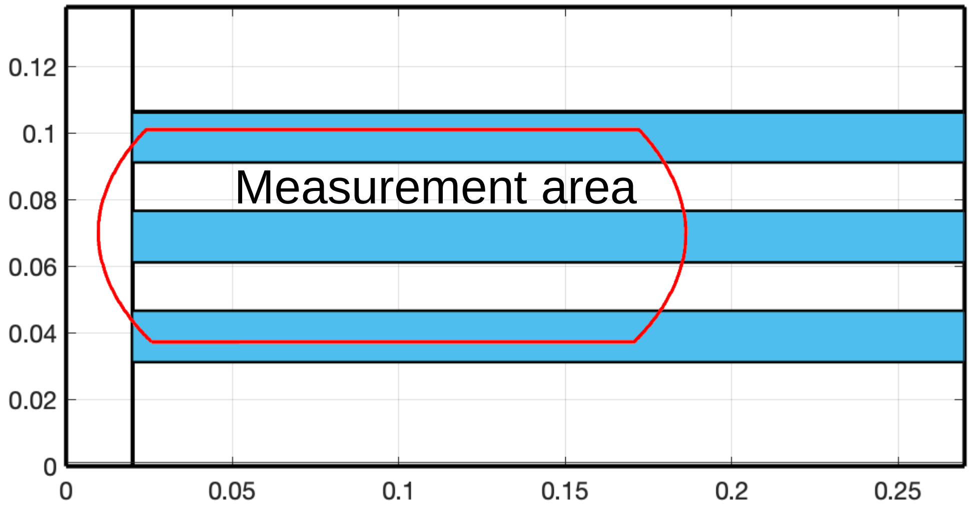

$t = 0$ s

Initial surface temperature

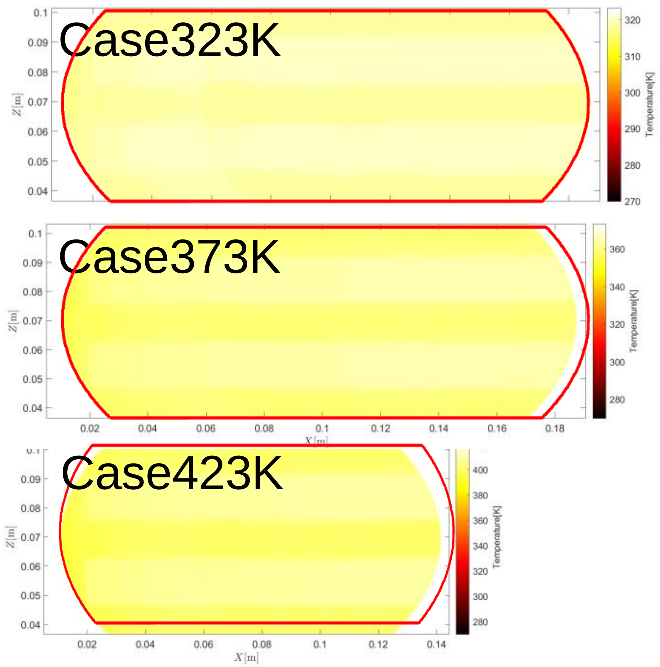

Prediction and measurement results

Measurement results

Material properties
- Steel
- Ceramic: Insulator
- Copper: Conductor

$t = 15\ s$

Case323K

Case373K

Case423K

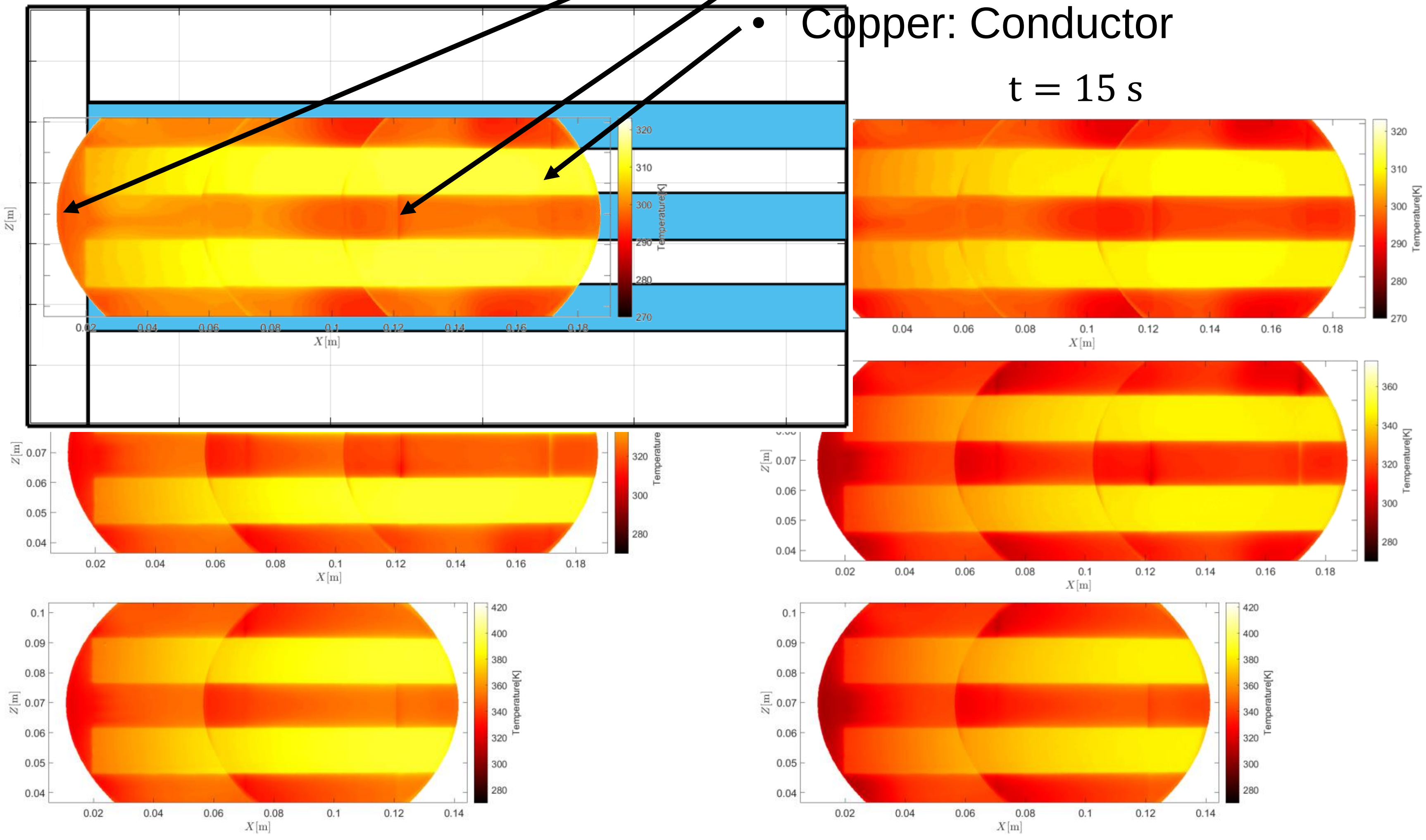

Prediction and measurement results

Transient temperature at Case323K

Thermal modelling

Experiment

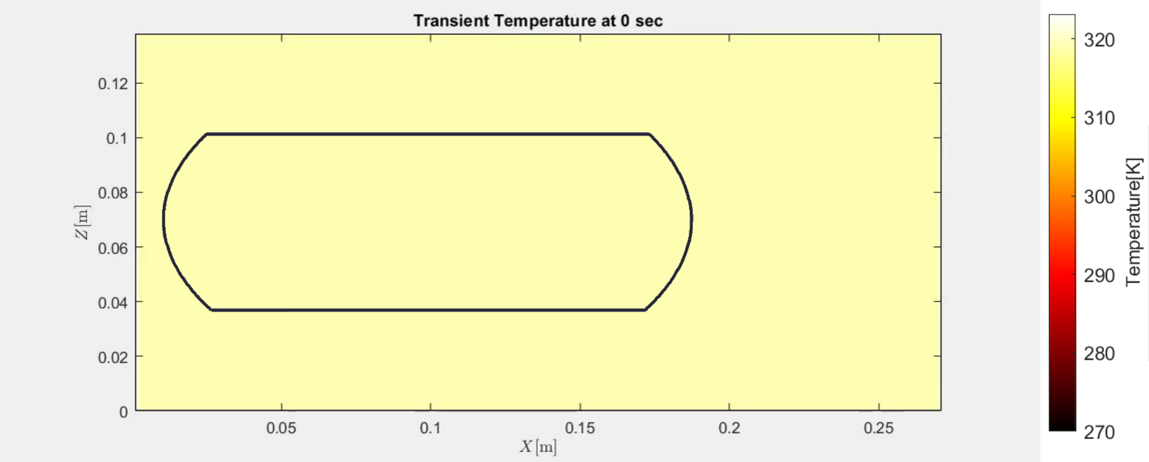

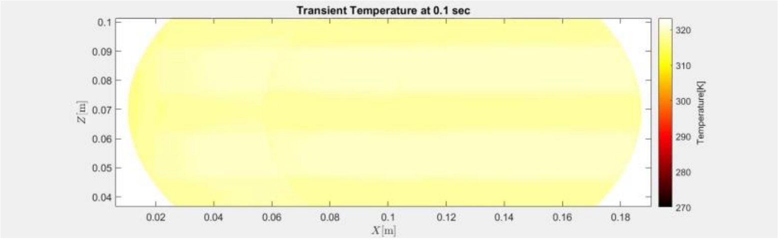

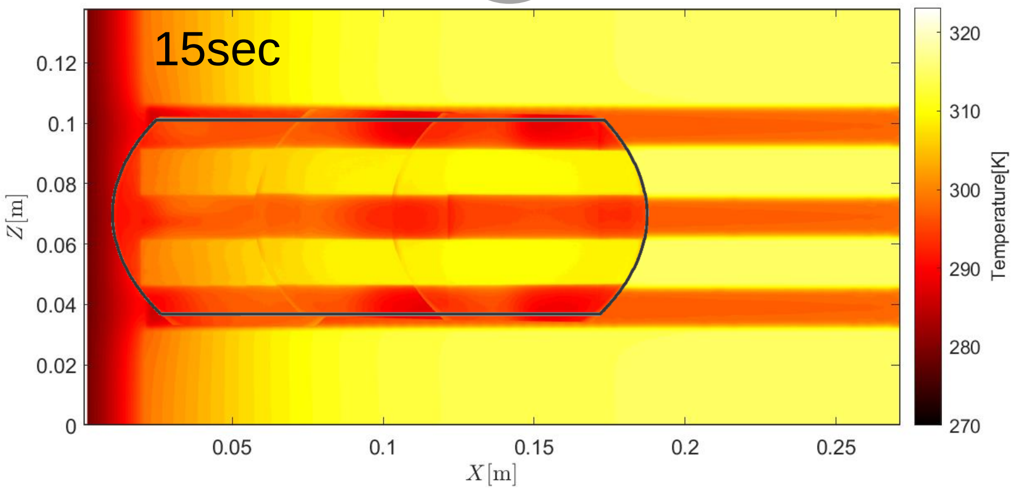

Prediction and measurement results

Overlaying experimental measurements & thermal modelling predictions

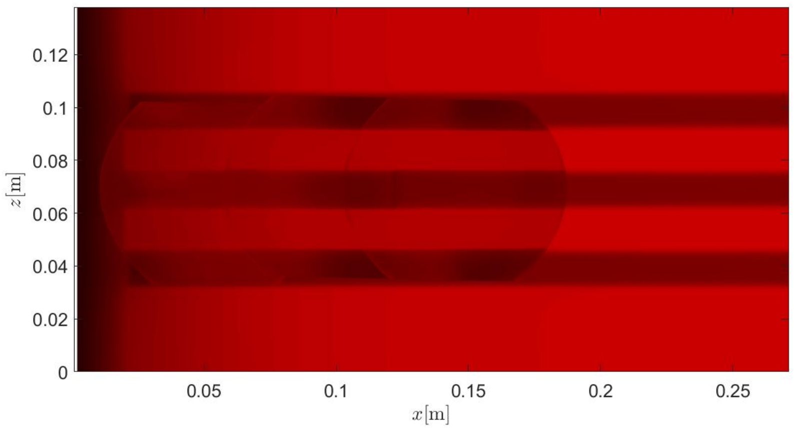

Case323K

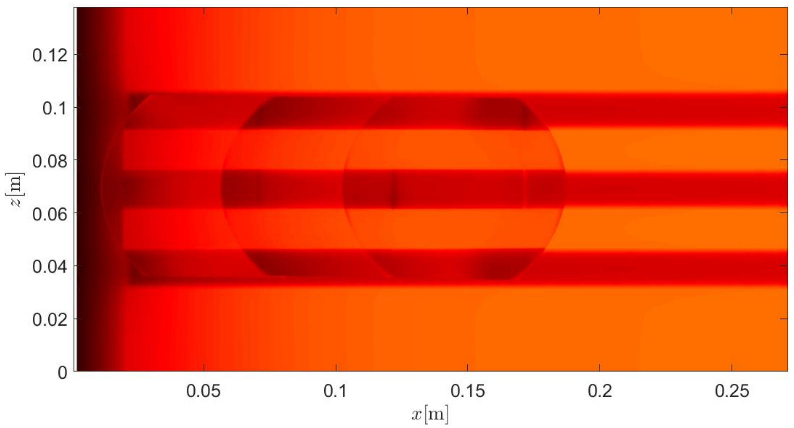

Case373K

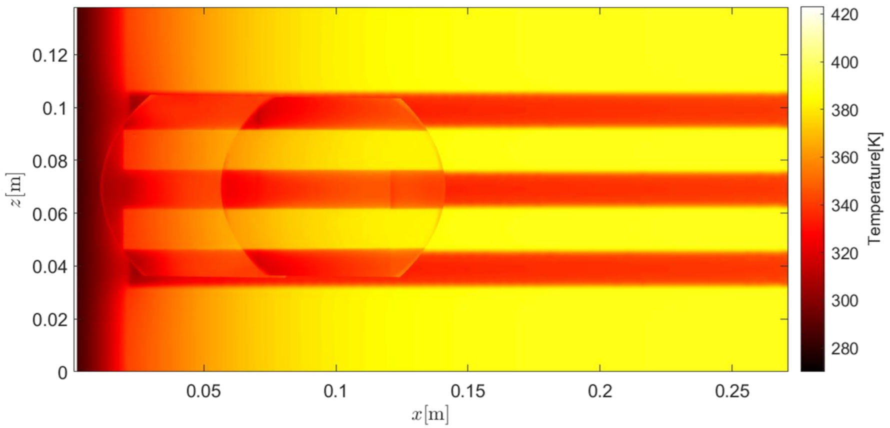

Case423K

Prediction and measurement results

Transient temperature along centreline at Case373K

3sec

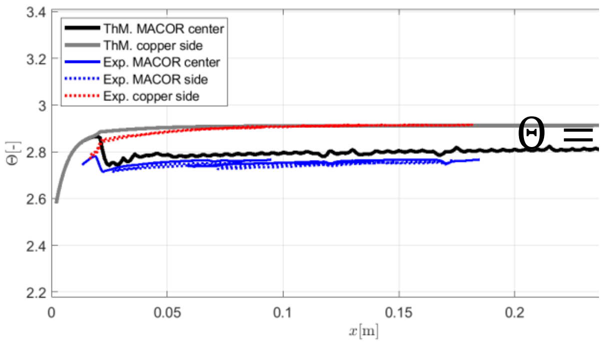

$$\Theta = \frac{T}{T_\infty}$$

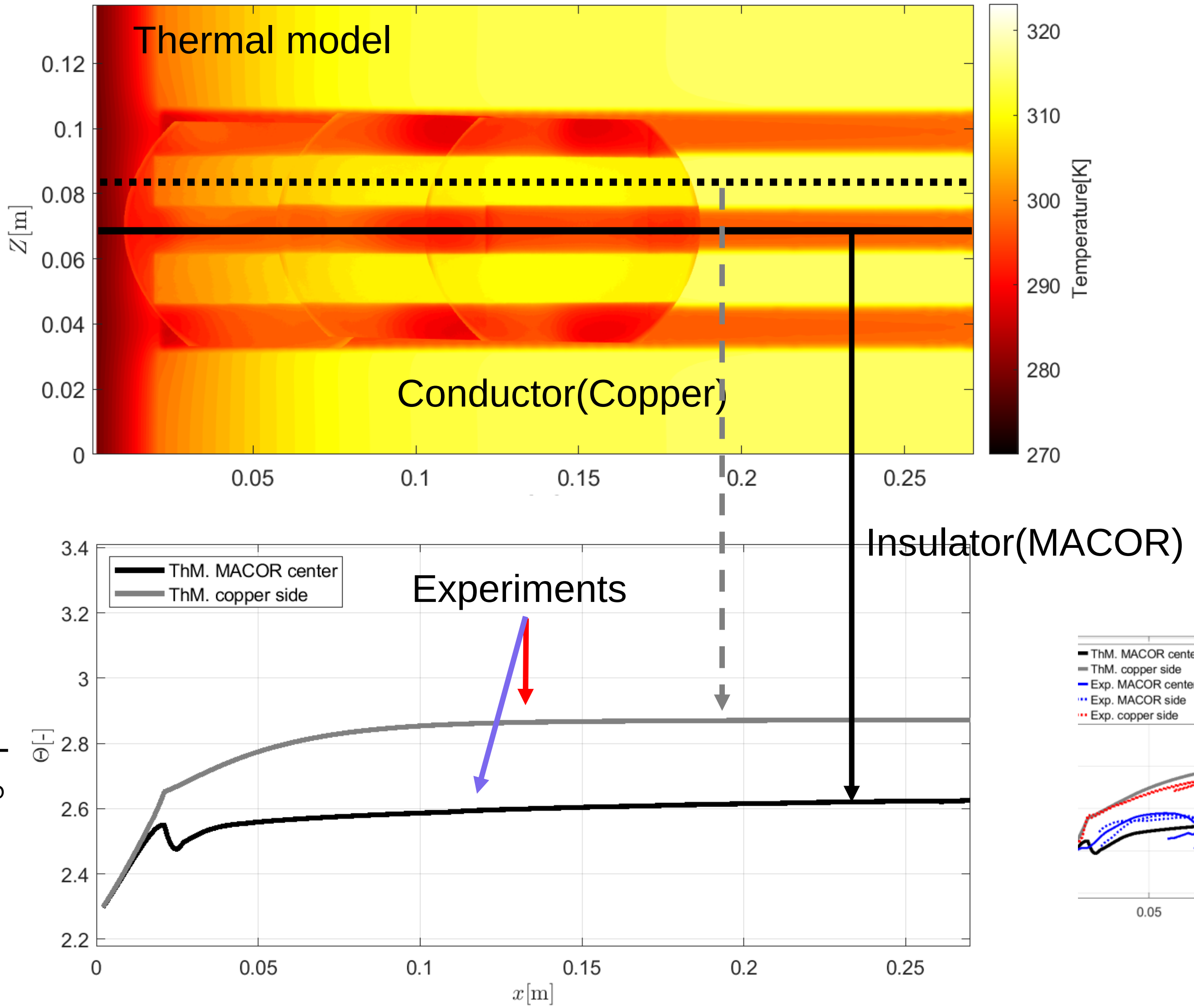

15sec

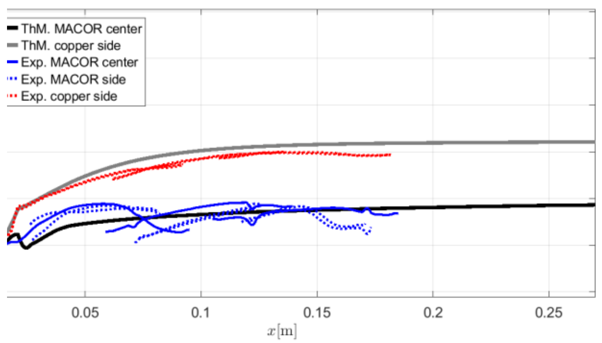

Prediction and measurement results

Transient temperature at all cases after t = 15 s

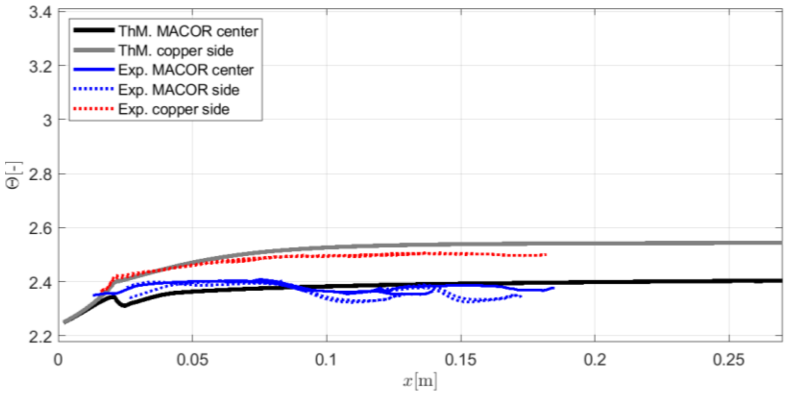

Case323K

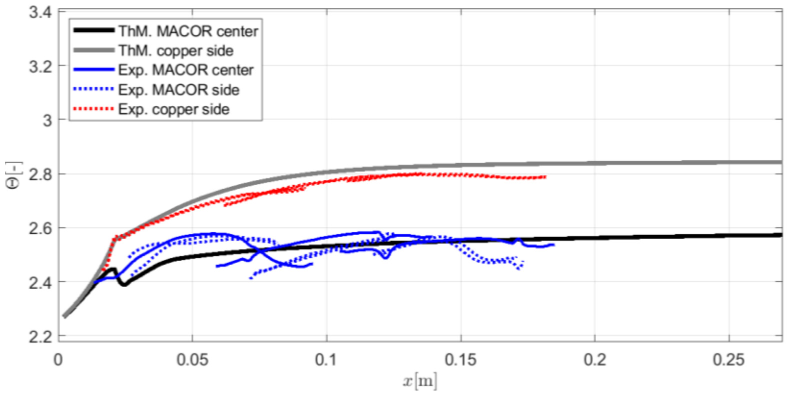

Case373K

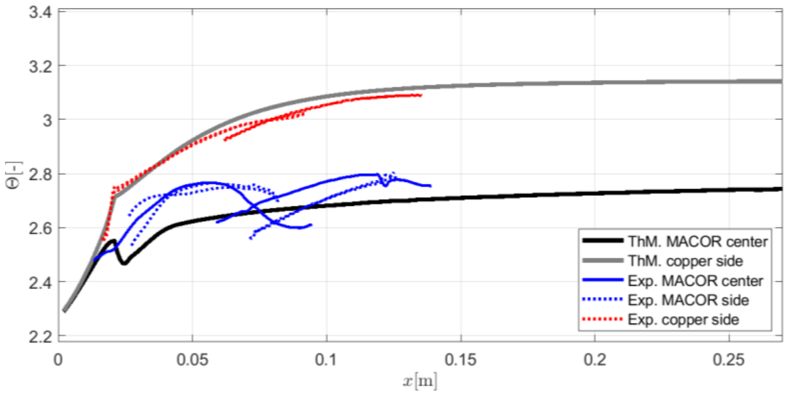

Case423K

Increase temperature difference

Prediction and measurement results

Transient temperature along spanwise after 15 s

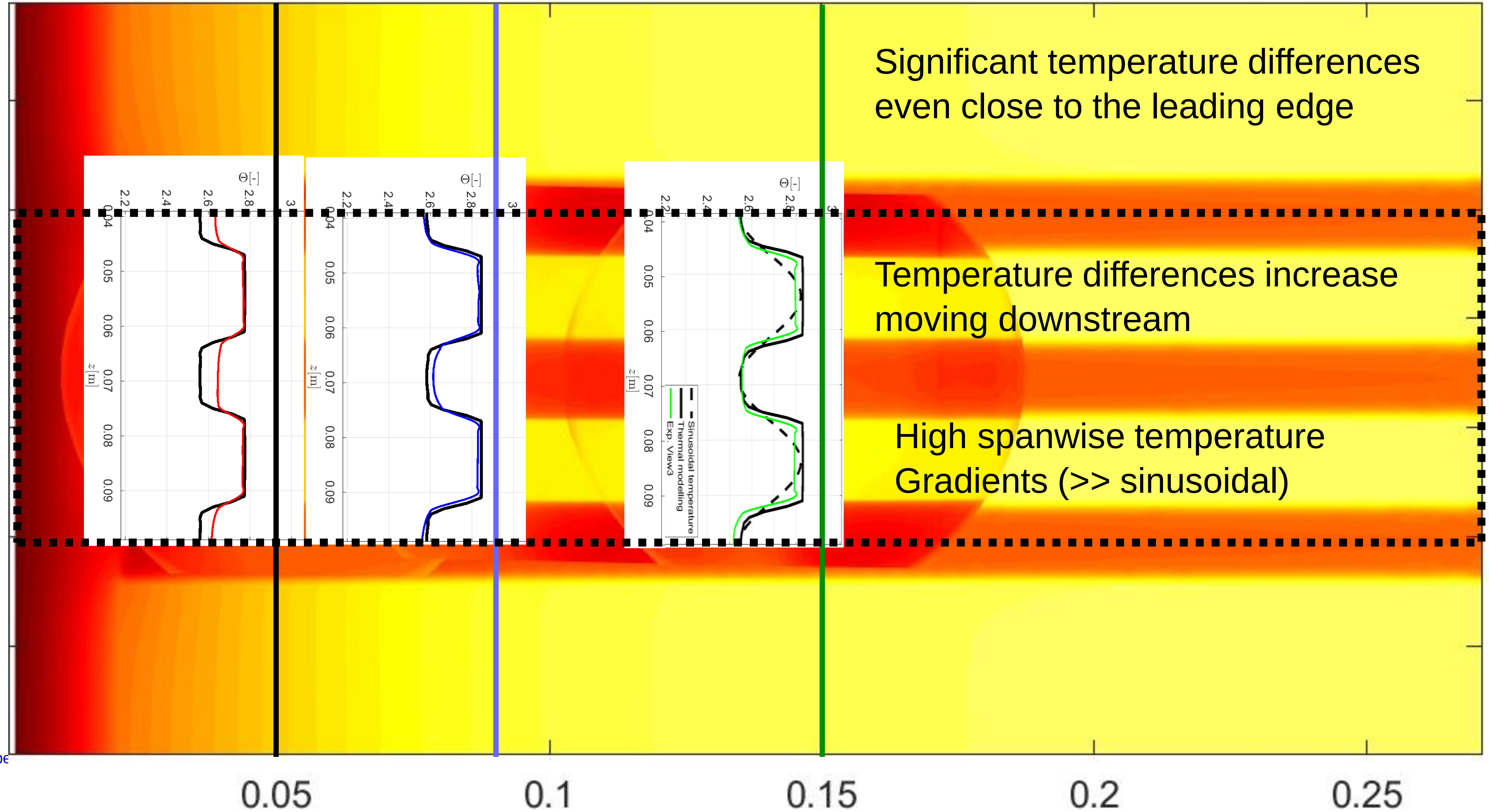

Prediction and measurement results

Transient temperature along spanwise after 15 s

Obvious temperature difference between the strips

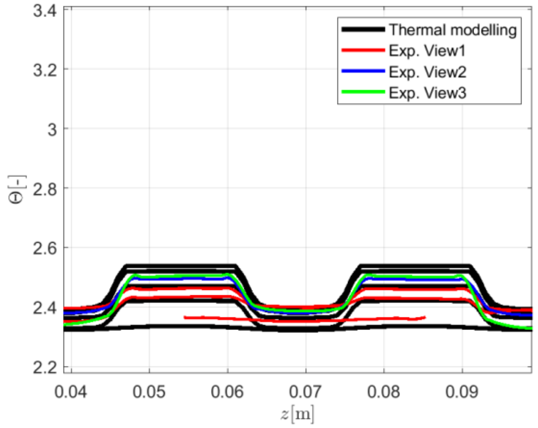

Case323K

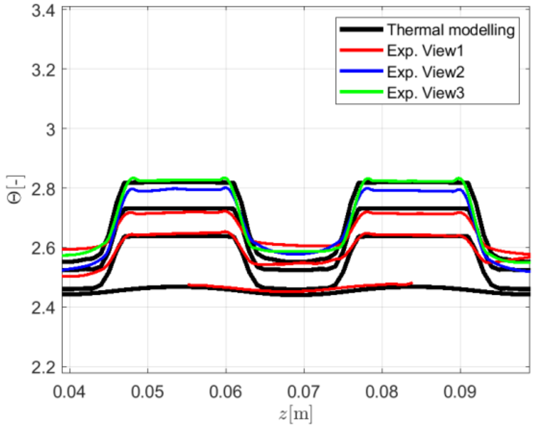

Case373K

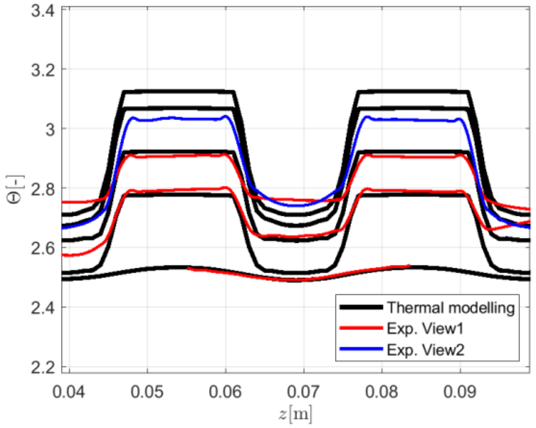

Case423K

Prediction and measurement results

Non-dimensional temperature difference after t=15s

$$\Theta = \frac{T}{T_\infty}$$

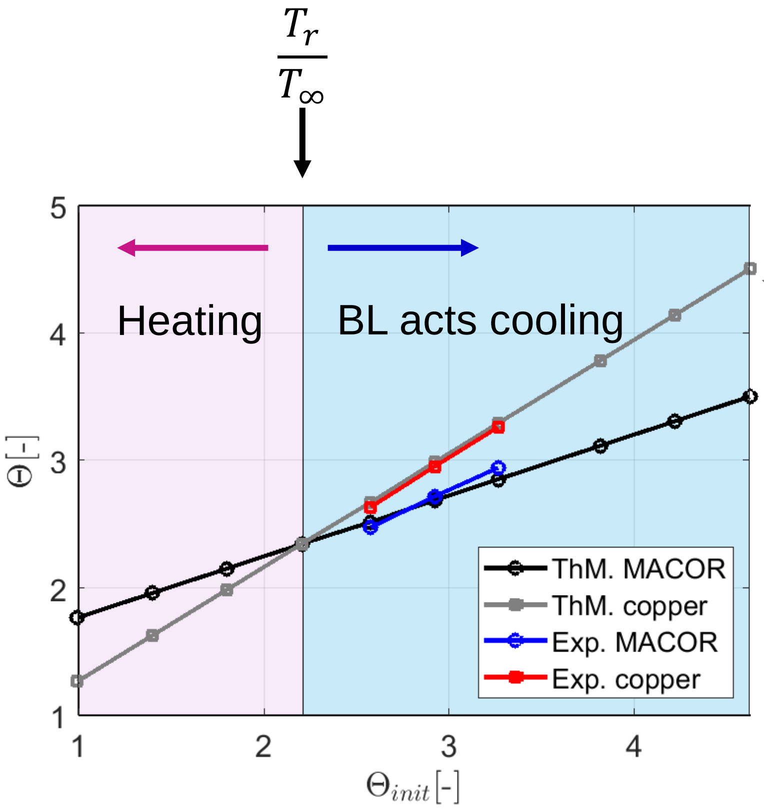

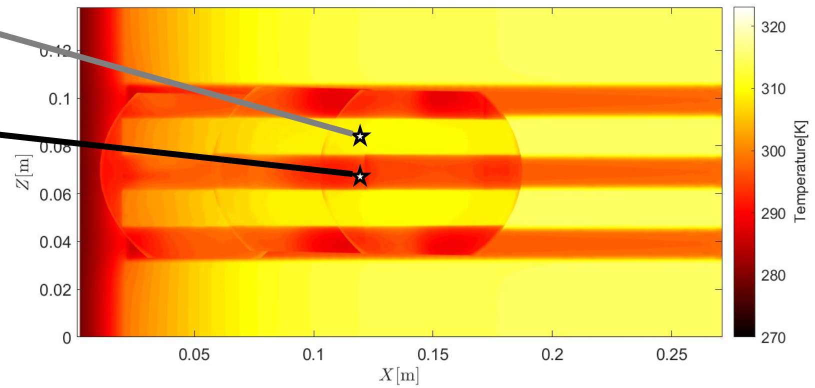

Streak Measurement

Current progress for setting up Laser Doppler Anemometry (LDA)

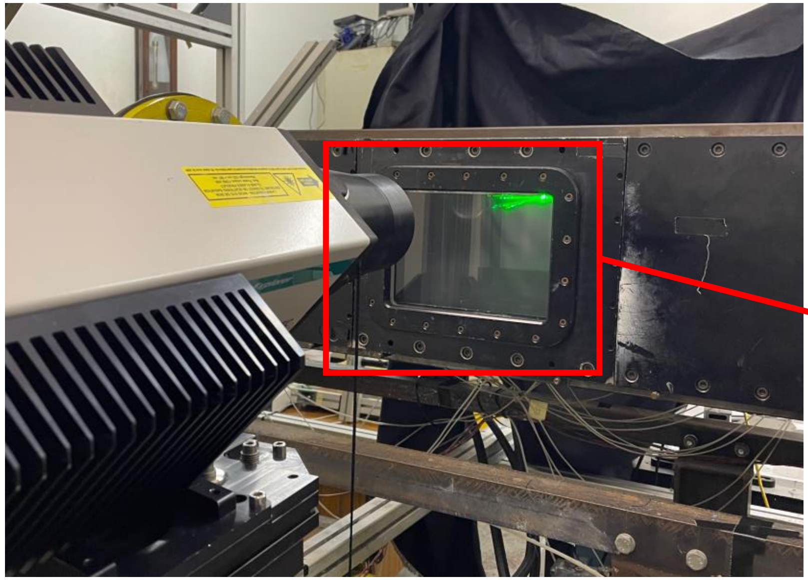

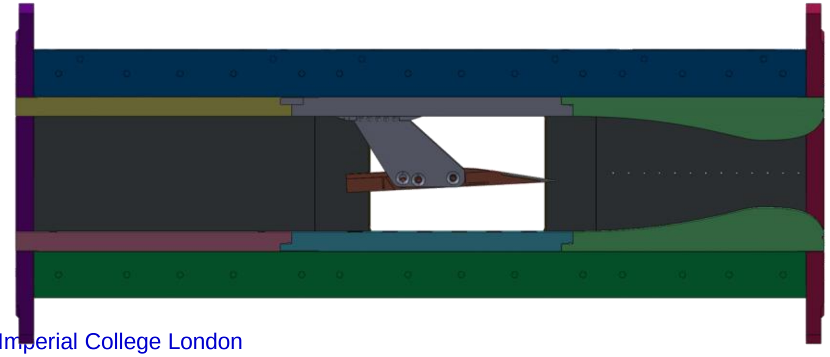

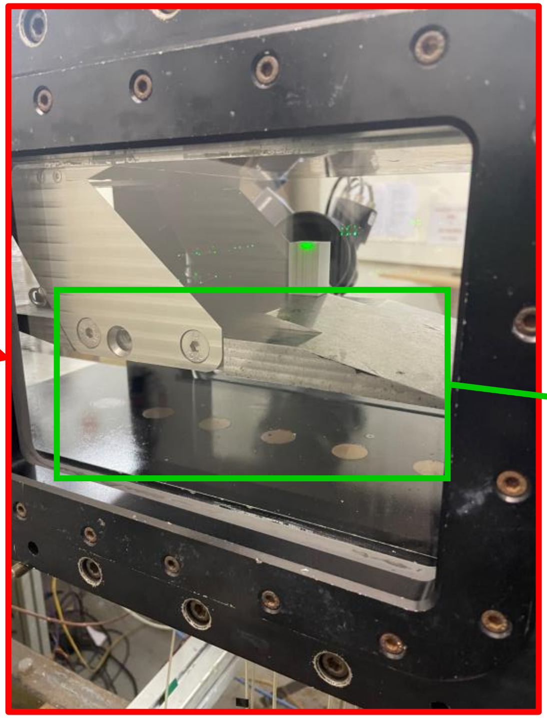

Streak Measurement
Preliminary results

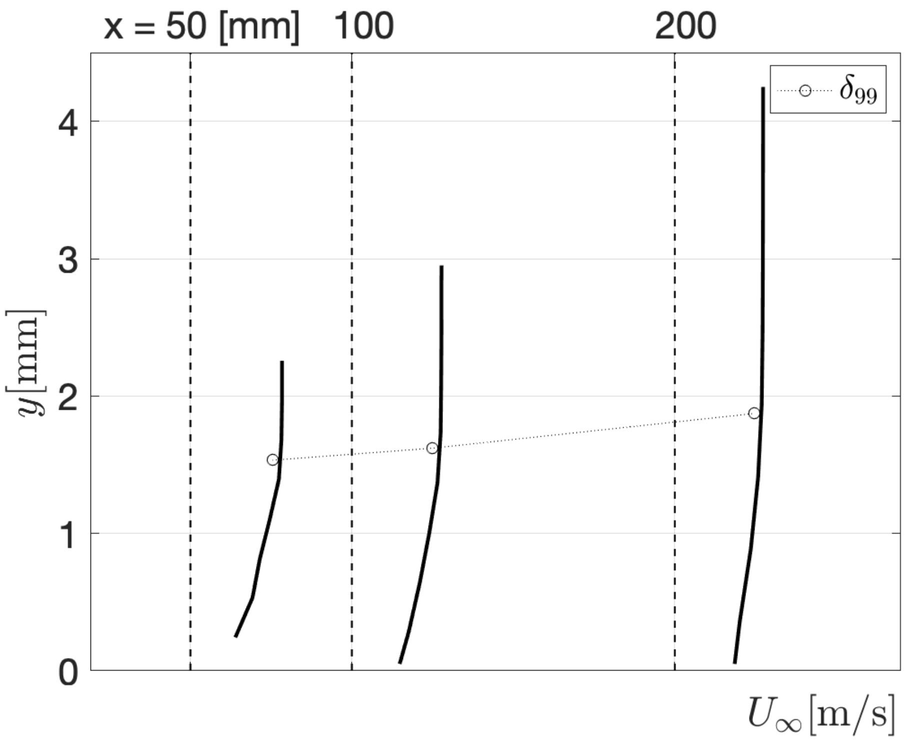

Background

Experimental setup and thermal modelling

Prediction and measurement results

Conclusion

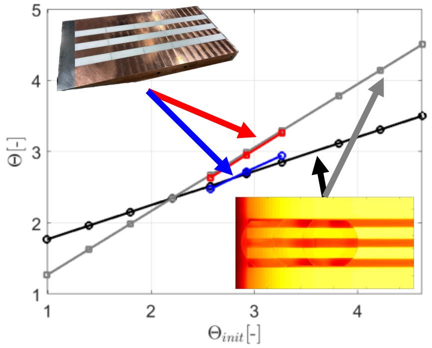

Conclusion

- Experiment and thermal modelling
  - Thermal modelling capturing a qualitative trend of the experiment
  - Higher Temperature difference can be achieved by higher initial temperature input
  - Temperature gradient becomes high between the insulator and the conductor
  - Global temperature distributions can be controlled by material properties and initial temperature

- Ongoing work
  - Conduction of Laser Doppler Anemometry (LDA) to quantify velocity for streaks

Concept

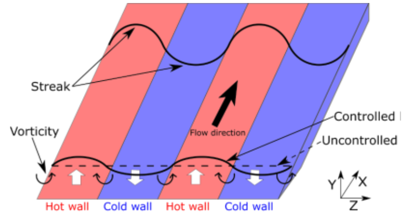

Preliminary design

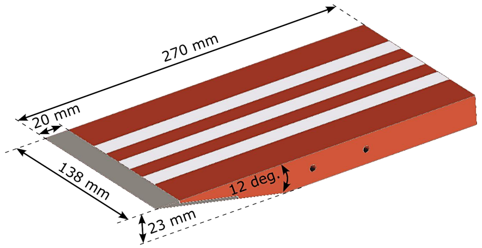

Temperature performance test

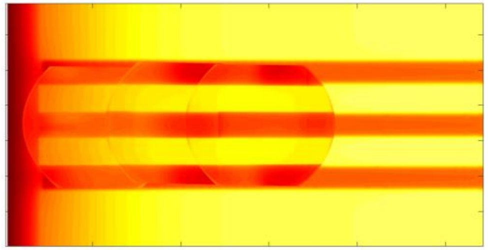

Streak performance test

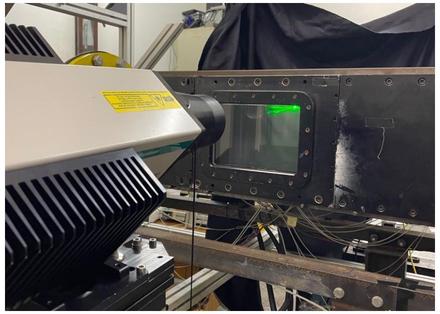

IMPERIAL

Spanwise non-uniform surface temperature distributions for high-speed boundary layer transition control

Dr Paul Bruce, Department of Aeronautics, Imperial College London

ERCOFTAC Autumn Festival, 10 October 2024

With credit to: **Kazuki Ozawa**, **Dr Luca Boscagli**
Funding from: Nakajima Foundation, QinetiQ (WSRF task 0105)
HPC time on ARCHER2 provided by EPSRC (UKTC)